CHAPTER III

THEORY

Zeolites

Zeolite are finding applications in many areas of catalysis and molecular sieve, generating interest in these materials in industrial and academic laboratories. As catalyst, zeolites exhibit appreciable acid activity with sharp-selectivity features not available in the compositional equivalent amorphous catalysts. In addition, these material can act as supports for numerous catalytically active metals. The porous framework of the zeolites enables them to act as molecular sieves i.e., they are used to separate molecular mixtures on the basis of size and shape molecule compounds or for the selective adsorption of gases. These unique properties are utilized in diverse industrial processes such as the purification of water as well as other liquids and gases, chemical separations, catalysis, and decontamination of radioactive wastes.

3.1 History of Zeolites

3.1.1 Early history [1]

The history of zeolites began in 1756 when the Swedish mineralogist Cronstedt discovered zeolite material, stilbite. He recognized zeolites as a new class of materials consisting of hydrated aluminosilicates of alkali and alkaline

earths. Because the crystals exhibited swelling and boiling when heated in a blowpipe flame, Cronstedt called the mineral a "zeolite" derived from two Greek words, "zeo" and "lithos" meaning "to boil" and "a stone". In 1777 Fontana described the phenomenon of adsorption on charcoal. In 1840 Damour observed that crystals of zeolites could be reversibly dehydrated with no apparent change in their transparency or morphology. Schafhautle reported the hydrothermal synthesis of quartz in 1845 by heating a "gel" silica with water in an autoclave. Way and Thompson (1850) clarified the nature of ion exchange in soils. Eichhorn in 1858 showed the reversibility of ion exchange on zeolite materials. St. Clarife Deville reported the first hydrothermal synthesis of a zeolite, levynite, in 1862. In 1896 Friedel developed the idea that structure of dehydrated zeolites consists of open spongy frameworks after observing that various liquids such as alcohol, benzene, and chloroform were occluded by dehydrated zeolites. Grandjean in 1909 observed that dehydrated chabazite adsorbs ammonia, air, hydrogen and other molecules, and in 1925 Weigel and Steinhoff reported the first molecular sieve effect. They noted that dehydrated chabazite crystals rapidly adsorbed water, methyl alcohol, ethyl alcohol and formic acid but essentially excluded acetone, ether or benzene. In 1927 Leonard described the first used of x-ray diffraction for identification in mineral synthesis. The first structures of zeolites were determined in 1930 by Taylor and Pauling. In 1932 McBain established the term "molecular sieve" to define porous solid materials that act as sieves on a molecular scale.

Thus, by the mid-1930's the literature described the ion exchange, adsorption, molecular sieve and structural properties of zeolite minerals as well as a number of reported synthesis of zeolites. The latter early synthetic work remains unsubstantiated because of incomplete characterization and the difficulty of experimental reproducibility.

Barrer began his pioneering work in zeolite adsorption and synthesis in the mid-1930's to 1940's. He presented the first classification of the then

know zeolites based on molecular size consideration in 1945 and in 1948 reported the first defined synthesis of zeolite including the synthetic analogue of the zeolite minerial merdenite.

3.1.2 Industrial history [1]

3.1.2.1 Synthetic zeolites

Barrer's in the mid late 1940's inspired of the Linde Division of Union Carbine Corporation to initiate studies in zeolite synthesis in search of new approaches for separation and purification of air. Between 1949 and 1954 R.M. Milton and coworker D.W. Breck discovered a number of commercially significant zeolites, type A, X and Y. In 1954 Union Carbide commercialized synthetic zeolites as a new class of industrial materials for separation and purification. The earliest applications were the drying of refrigerant gas and nature gas. In 1955 T.B. Reed and D.W. Breck reported the structure of synthesis zeolite A. In 1959 Union Carbide marketed the "ISOSIV" process for normal-isoparaffin separation, representing the first major bulk separation process using true molecular sieving selectivity. Also in 1959 a zeolite Y-based catalyst was marketed by Carbide as an isomerization catalyst.

In 1962 Mobil Oil introduced the use of synthetic of zeolite X as a cracking catalyst. In 1969 Grace described the first modification chemistry based on steaming zeolite Y to form an "ultrastable" Y. In 1967-1969 Mobil Oil reported the synthesis of the high silica zeolites beta and ZSM-5. In 1974 Henkel introduced zeolite A in detergents as a replacement for the enviromentally suspect phosphates. By 1977 industry-wide 22,000 tons of zeolite Y were in use in catalytic cracking. In 1977 Union Carbide introduced zeolite for ion-exchange separations.

3.1.2.2 Natural zeolites [1]

For 200 years following their discovery by Cronsted, zeolite minerial (or natural zeolite) were considered to occur typically as minor constituent in cavities in basaltic and volcanic rock. Such occurrences precluded their being obtained in mineable quantities for commercial use. From 50' s to 1962 major geologic discoveries revealed the widespread occurrence of a number of natural zeolites in sedimentary deposits throughout the Western United States. The discoveries resulted from the use of x-ray diffraction to examine very fine-grained (1-5 μm) sedimentary rock. Some zeolites occur in large near monomineralic deposits suitable for mining. Those that have been commercialized for adsorbent applications include chabazite, erionite, modernite and clinoptilolite.

3.2 Structural of Zeolite

Zeolites are crystalline aluminosilicates of group IA and IIA elements such as sodium, potassium, magnesium, and calcium.

Chemically, they are represented by the empirical formular : [1]

$$M_{2/n}O.Al_2O_3.ySiO_2.wH_2O$$

where y is 2 to 10, n is the cation valence, and w represents the water contained in the voids of the zeolite. Structurally, zeolites are complex, crystalline inorganic polymer based on an infinitely extending three- dimensional, four-connected framework of AlO_4 and SiO_4 tetrahedra (Figure 3.1) linked to each other by the sharing of oxygen ions. Each AlO_4 tetrahedron in the framework bears a net negative charge which is balanced by a cation. The framework structure contain channels or interconnected voids that are occupied by the cations and water molecule. The cations are mobile and ordinary undergo ion exchange. The water may be removed reversibly, generally by the application of heated, which leaves intact a crystalline host structure permeated

by the micropores and voids which may amount to 50% of the crystals by volume.

The structural formula of zeolite is based on the crystallographic unit cell, the smallest unit of structure, represented by : [1]

$$M_{x/n}[(AlO_2)_x(SiO_2)_y].wH_2O$$
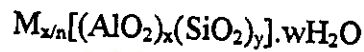
where n is the valence of cation M, w is the number of water molecules per unit cell, x and y are total number of tetrahedra per unit cell, and y/x usually has values of 1 to 5. In the case of high silica zeolites y/x is 10 to 100.
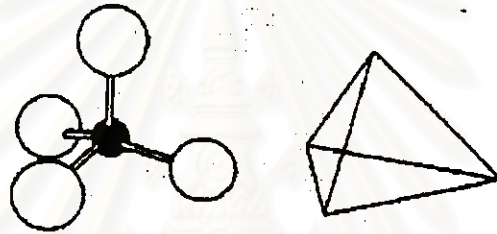

Figure 3.1 SiO_4 or AlO_4 tetrahedra [2].

In most zeolite structures the primary structural units, the AlO_4 or SiO_4 tetrahedra, are assembled into secondary building units (SBU). The final structure framework consists of assemblages of secondary units.

A secondary building unit consists of selected geometric groupings of those tetrahedra, which can be used to describe all of known zeolite structures. These secondary building unit consist of 4(S4R), 6(S6R) and 8(S8R)-member single ring, 4-4(D4R), 6-6(D6R), 8-8(D8R)-member double ring, and 4-1, 5-1, 4-4-1 branch ring [3]. The topologies of these units are shown in figure 3.2 Also listed are the symbols used to describe them. Most zeolite framework can be generated from several different SBU's. Description of known zeolite structures based on their SBU's are listed in Table 3.1 [3]. Both zeolite ZSM-5 and ferrierite are described by their 5-1 building units. Offertile, zeolite L,

cancrinite, and erionite are generated using only single 6-member rings. Some zeolite structures can be described by several units.
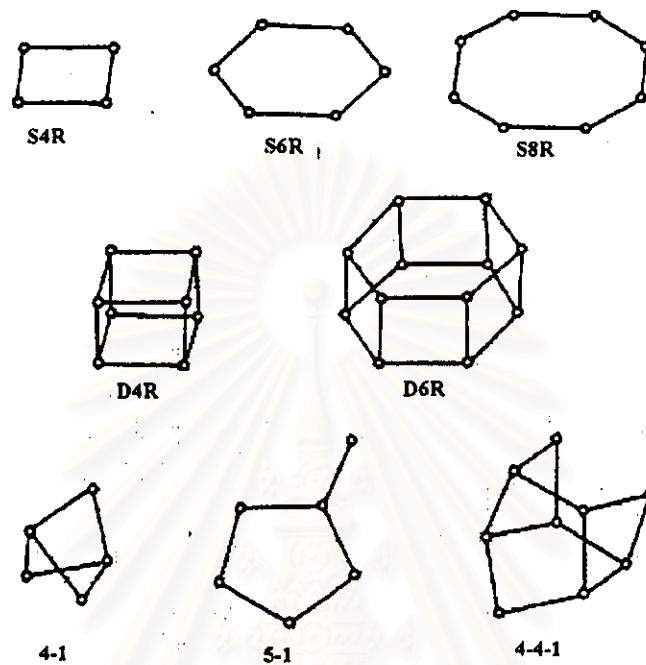

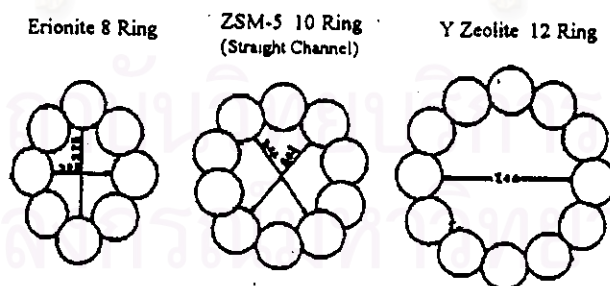Figure 3.2 Secondary building units (SBU's) found in the zeolite structures [3].

Figure 3.3 Typical zeolite pore geometries [5].

Table 3.1 Zeolites and their secondary building units. The nomenclature
used is consistent with that presented Figure 3.2 [4].

ZEOLITE	SECONDARY BUILDING UNITS
	4	6	8	4-4	6-6	8-8	4-1	5-1	4-4-1
Bikitaite								X	
Li-A (BW)	X	X	X						
Analcime	X	X							
Yugawaralite	X		X						
Episitbite								X	
ZSM-5								X	
ZSM-11								X	
Ferrierite								X	
Dachiardite								X	
Brewsterite	X								
Laumonite		X							
Mordenite								X	
Sodalite	X	X							
Henulandite									X
Stibite									X
Natrolite							X		
Thomsonite							X		
Edingtonite							X		
Cancrinite		X							
Zeolite L		X							
Mazzite	X								
Merlinoite	X		X			X			
Philipsite Zeolite	X		X						
Losod		X							
Erionite	X	X							
Paulingite	X								
Offretite		X							
TMA-E (AB)	X	X							
Gismondine	X		X						
Levyne		X							
ZK-5	X	X	X		X				
Chabazite	X	X			X				
Gmelinite	X	X	X		X				
Rho	X	X	X			X			
Type A	X	X	X	X					
Faujasite	X	X			X				

The catalytically most significant are those having pore opening characterized by 8-, 10-, 12-rings of oxygen atoms. Some typical pore geometries are shown in figure 3.3 [5].

3.2.1 Small pore zeolites

Structures of some small pore zeolite are illustrated in Figure 3.4. The erionite structure, Figure 3.4 (a), is hexagonal containing "supercage" supported by column of cancrinite units linked through double 6 rings. Access to, and between, The supercages is gained through 8 rings.

In the chabazite framework, Figure 3.4(b), the double rings layer sequence is ABCABC, and the double 6 ring units are linked together though titled 4 ring units. The framework contains large ellipsoidal cavities, Figure 3.4 ©, each entered though six 8 ring units. These cavities are joined via their 8 ring units, forming a 3 dimensional channel system.

3.2.2 Medium pore zeolites

The channel system of zeolite ZSM-5, represented in Figure 3.5, shows a unique pore structure that consists of two intersecting channel systems: one straight (5.4*5.6 A°) and other sinusoidal (5.1*5.4 A°) and perpendicular to the former. Both channel systems have ten-membered ring elliptical openings.

3.2.3 Large pore zeolites

Mordenite, Figure 3.6 (a), is characterized by a one dimensional system of parallel ellipticals channels, defined by 12 oxygen ring.

The faujasite structure, Figure 3.6 (b), is built up of truncated octahedra interconected via double 6 ring units. Faujasite contains extremely large supercages (~13 A° diameter) entered through 12 oxygen ring.
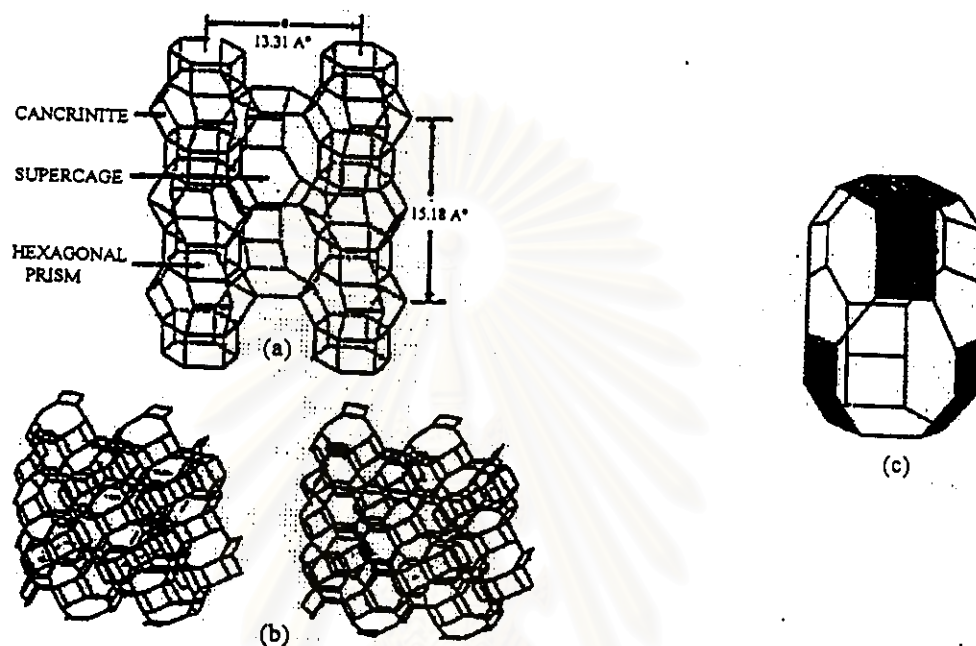

Figure 3.4 Small pore zeolites (a) Erionite framework
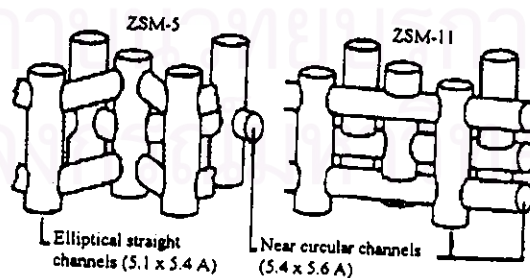(b) Chabazite framework © Chabazite cavity [5].

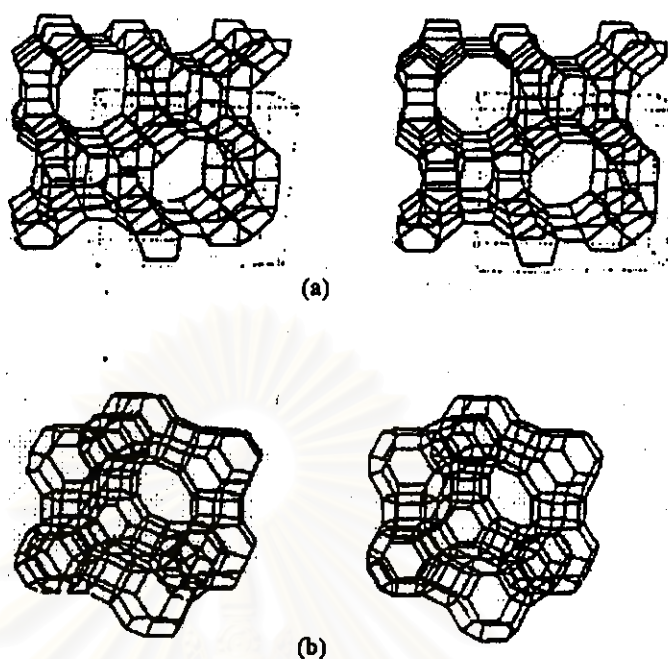
Figure 3.5 ZSM-5 and ZSM-11 chanel system [5].

(a)

(b)

Figure 3.6 Large pore zeolites

(a) Mordenite framework

(b) Faujasite framework [5].

3.3 X and Y Zeolite Structures [6]

X zeolite, Y zeolite and faujasite have topologically similar structures. They differ in their characteristic silica-to-alumina ratios and consequently differ in their crystal-lattic parameter, with a variation of about 2 percent over the range of permissible Si/Al ratios. They also differ in properties as cation composition, cation location, cation exchangeability, thermal stability, adsorptive and catalytic character.

In the X and Y zeolites and faujasite, the silica and alumina tetrahedra are joined together to form a cuboctahedron, as shown in figure 3.7. This unit.

referred to as a sodalite unit or truncated octahedron, contains 24 silica and alumina tetrahedra. The sodalite unit is the secondary building block of a number of zeolites, including sodalite, zeolite A, zeolite X, zeolite Y and faujasite. Molecules can penetrate into this unit through the six-membered oxygen rings, which have a free diameter 2.6 °A; the unit contains spherical void volume with 6.6 °A free diameter. Since the pore diameter is so small, only very small molecules, e.g., water, helium, hydrogen, or ions can enter the sodalite cage.
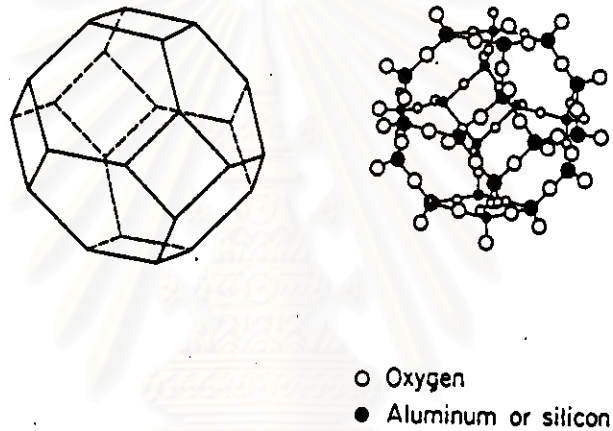

o Oxygen
● Aluminum or silicon

Figure 3.7 Sodalite cage structure. A formal representation of a truncated octahedron is shown on the left, and individual atoms are indicated on the right; the lines in the structure on the left represent oxygen anions, and the points of intersection represent silicon or aluminum ions [6].

The unit cell of the faujasite-type zeolite is cubic which a unit-cell dimension of 25 °A, and it contains 192 silica and alumina tetrahedra. The unit cell dimension varies with Si/Al ratio. Each sodalite unit in the structure is connected to four other sodalite unit by six bridge oxygen ions connecting the hexagonal faces of two units, as shown in figure 3.8. The truncated octahedra are stacked like carbon atom in a diamond. The oxygen bridging unit is

referred to as a hexagonal prism, and it may be considered another secondary unit. This structure results in a supercage (sorption cavity) surrounded by 10 sodalite unit which is sufficient large for an inscribed sphere with a diameter of 12 °A. The opening into this large cavity is bounded by 6 sodalite units, resulting in a 12-member oxygen ring with a 7.4 °A free diameter. Each cavity is connected to four other cavities, which in turn are themselves connected to three additional cavities to form a highly porous framework structure.
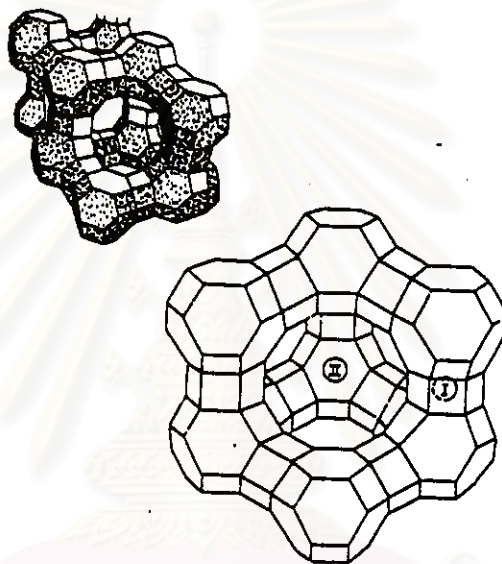

Figure 3.8 Perspective views of the fuajasite structure. The silicon or aluminum ions are located at the corner and the oxygen ions near the edges. Type I and II sites are indicated; the supercage is in the center [6].

This framework structure is the most open of any zeolite and is about 51 percent void volume, including the sodalite cage; the supercage volume represents 45 percent of the unit cell volume. The main pore structure is three-dimensional and large enough to admit large molecules, e.g., naphtalene and fluorinated hydrocarbon. It is within the pore structure that the locus of catalytic activity resides for many reactions. A secondary pore structure

involving the sodalite unit exists but its apertures are too small to admit most molecules of interest in catalysis.

3.4 Zeolites as Catalysts [2]

The first use of zeolite as catalysts occurred in 1959 when zeolite Y was used as an isomerization catalyst by Union Carbide. More important was the first use of zeolite X as a cracking catalyst in 1962, based upon earlier work by Plank and Rosinski. They noted that relatively small amounts of zeolites could be incorporated into the then-standard silica/alumina or silica/clay catalysts. The use of zeolite in this way as promoters for petroleum cracking greatly improved their performance.

3.4.1 Potential versatility of zeolites as catalysts

Vaughan has graphically described zeolites as "molecules boxes" which have variable dimensions suited to the encouragement of molecular rearrangements inside their confined geometry. The conditions inside the "box", and of box itself, can be controlled in a variety of ways based upon the unique properties of zeolite frameworks as summarized in Table 3.2 .

3.4.1.1 Crystal voidage and channels

Although some heterogenous reactions will take place at the external crystal surface, most practical zeolite catalysis takes place inside the framework. Here zeolites have the advantage of a vary large internal surface, about 20 times larger than their external surface for the more open framework (e.g. zeolite X and Y). This internal capacity provides the appropriate surfaces at which catalytic transformation can take place. In the faujasite zeolite is typically in the series of large cavities easily available via three-dimensional open-pore networks.

Further flexibility which is useful for planned catalytic uses arises in the more recently produced zeolites with subtle different cavity and channel systems. ZSM-5, for instance, has a three-dimensional system linked via intersections rather than cavities and mordenite catalysis seems to take place only in the largest channels.

Table 3.2 Correlation between zeolite properties and catalytic functionality [2].

Property	Catalytic Functionality
Crystal voidage and channels	Extensive internal surface to encourage catalytic processes
Variable pore size	Creates both reactant and product selectivity via molecules seiving
Ion exchange	Catios (i) control pore size, (ii) create high potential energy field within voidage (active site) and (iii) enable distribution of catalytically active metals on the zeolite substrate
Salt occlusion	Controls pore size, provide another method of metal incorporation and can improve thermal stability and poisoning resistance
Framework modification	Varies lattice change (by synthesis or modification) to enchance active site production and thermal stability

3.4.1.2 Variable pore sizes

Given that catalytic takes place largely within zeolite framework, access to this environment is patently controlled by oxygen windows. This is diffusion limited process, as is the effect of product molecules after transformations have

taken place. This means that zeolites have very special practical advantages over the more traditional catalysts, in that admit only certain reactant molecules and this can be potentially tailored to produced selected product. This selectivity is known as "sharps-selective catalysis" and controlled by "configurational diffusion" -this phase was coined by Weiss to express a diffusion regiment in which useful catalytic reactions and promoted by virtue of a matching of size, sharp and orientation of the reactant product molecules to the geometry of zeolitic framework.

3.4.1.3 Ion exchange

Perhaps more relevant is the way in which ion exchange can be employed to place cations into very specific framework sites so as to create small volumes of high electrostatic filed. These fields are "active sites" to which an organic reactant molecule can be attracted thus promoting the bond distortion and rupture essential to molecular rearrangements.

Another feature of ion exchange is that it provides a route for the introduction of metal cations with a view to their subsequent reduction to metal particles. These exist in the so-called "bifunctional" zeolite catalysts used to effect both hydrogenation and dehydrogenation reactions.

3.4.1.4 Salt occlusion

The introduction of a salt molecule into a zeolite can be the first stage in the incorporation of a metal for subsequent reduction as mentioned above. It can also be used to enhance thermal stability. Yet another purpose is to "pacify" zeolite cracking catalysts. The problem here is that crude oil contain metal cations (Ni, Cu, V, Fe) originating from the metal porphyrins thought to play an inherent part in the geological formation of oil. These metals create

unwanted reactivity causing carbon (coke) formation and subsequent loss of catalytic properties. The occlusive introduction of stannates, bismuthatrs, or antimonates pacifies these metals to extend useful catalyst bed lift. It enables the refinery to cope whit a variety of crude oil from different oil fields and illustrates the flexible technology which can be achieved in zeolite catalysis.

Other salt treatment, via phosphates or fluorides, have been used to improve performance.

3.4.1.5 Framework modification

The electrostatic field of zeolite can be manipulated by isomorphous substitution into framework Si and Al sites. This can be done by synthetic or modification routes. When the Si:Al ratio is close to 1 the field strength is at its highest as is the cation content - i.e. the conditions of maximum negative charge on the framework. An increase of the Si:Al causes a greater separation of negative charge and hence higher field gradients (obviously also condition by cation position and cation types). IN this way, the catalytic activity can be controlled, and alter parameters altered. A well known example of these effects is the way in which the thermal and chemical stabilities of synthetic faujasite can be critically altered by aluminum removal.

Framework substitution also can be created by the introduction of atoms other than Si and Al into tetrahedral sites via synthesis or modification. The ZSM-5 can accept B and Ga into tetrahedral sites by simple salt treatment as mentioned earlier, although a similar reaction in other frameworks is by no means as facile.

3.5 Zeolite Active sites

3.5.1 Acid sites

Classical Bronsted and Lewis acid models of acidity are used to classify the active sites on zeolites. Bronsted acidity is proton donor activity; a tridiagonally co-ordinated alumina atom is an electron deficient and can accept an electron pair, therefore as a Lewis acid [7, 8].

In general, the increase in Si/Al ratio will increase acidic strength and thermal stability of zeolite [9]. Since the number of acidic OH groups depend on the number of aluminum zeolite ,s framework, decrease in Al content is expected to reduce catalytic activity of zeolite. If the effect of increase in the acidic centers, increase Al content, shall result in enhancement of catalytic activity.

Based on electrostatic consideration, the charge density at a cation site increases with increasing Si/Al. It was conceived that these phenomena are relate to reduction of electrostatic interaction between framework sites, and possibly to difference in the order of aluminum in zeolite crystal-the location of Al in crystal structure [8].

Recently it has been reported the mean charge on proton was shifted regularly towards higher values as the Al content decreased [7]. Simultaneously the total number of acidic hydroxyls, governed by the Al atoms, were decreased. This evidence emphasized that the entire acid strength distribution (weak, medium, strong) was shifted towards stronger values. That is the weaker acid sites become stronger with the decrease in Al content.

An important in thermal and hydrothermal stability has been described to the lower density of hydroxyls groups which is parallel to the Al content [7].

A longer distance between hydroxyl groups decreases the probability of dehydrogenation that generates defects on structure of zeolites.

3.5.2 Generation of acid centers

Protonic acid centers of zeolite are generated in various ways. Figure 3.9 depicts the thermal decomposition of ammonium exchanged zeolites yielding the hydrogen form [3].

The Bronsted acidity due to water ionization on polyvalent cations, described below, is depicted in figure 3.10 [10].

$$M^{n+} + xH_2O \rightarrow M(OH)_x^{(n-x)+} + xH^+ \qquad (3.1)$$
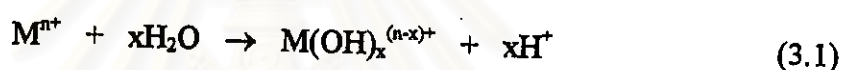
The exchange of monovalent ions by polyvalent cations could improve the catalytic property. Those highly charged cations create very acidic centers by hydrolysis phenomena.

The Bronsted acid sites are also generated by the reduction of transition metal cations. The concentration of OH groups of zeolite containing transition metals was noted to increase by reduction with hydrogen at 250-450 ^{0}C to increase with the rise of the reduction temperature [10].

$$Cu_2+ + H_2 \rightarrow Cu^0 + 2H^+ \qquad (3.2)$$
$$Ag^+ + 1/2H_2 \rightarrow Ag^0 + H^+ \qquad (3.3)$$
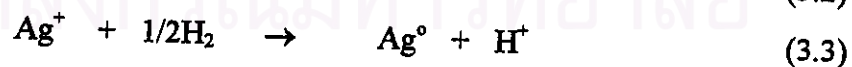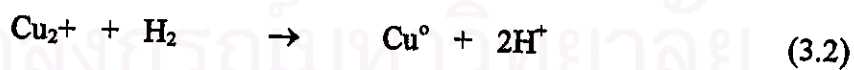
The formation of Lewis acidity from Bronsted sites is depicted in Figure 3.12 [10]. The dehydration reaction decreases the number of protons and increases that of Lewis sites.
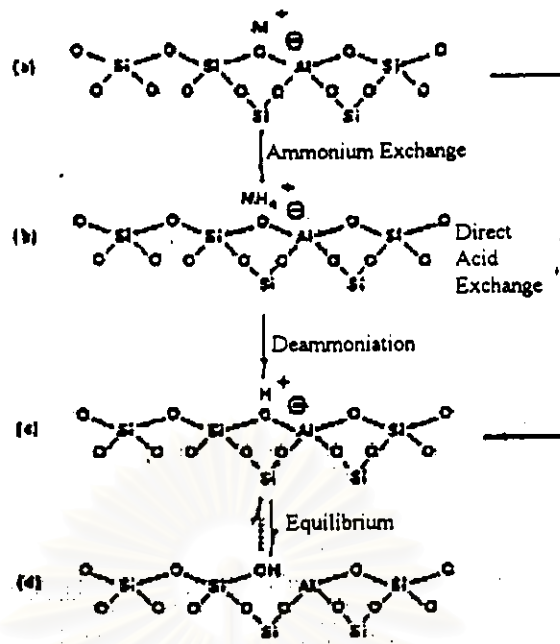
Figure 3.9 Diagram of the surface of a zeoilte framework

(a) In the as-synthesized from M^+ is ether an organic cation or an alkali metal cation.

(b) Ammonium in exchange produces the NH_4^+ exchanged form.

(c) Thermal treatment is used to remove ammonia, producing the H^+, the acid form.

(d) The acid form in © is the equilibrium with the form shown in (d), where there is the silanol group adjascent to a tricoordinate aluminium [3].
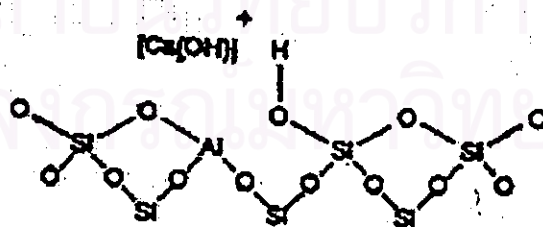

Figure 3.10 Water molecules coordinate to polyvalent cation are dissociated by heat treatment yielding Bronsted acidity [10].

Bronsted (OH) and Lewis (-Al-) sites can be present simultaneously in the structure of zeolite at high temperature. Dehydroxylation is though to occur in ZSM-5 zeolite above 500 °C and calcination at 800-900 °C produces irreversible dehydroxylation which causes defection in crystal structure of zeolite.

Dealumination is believed to occur during dehydroxylation which may result from the steam generation within the sample. The dealumination is indicated by an increases in the surface concentration of aluminum on the crystal. The dealumination process is expressed in Figure 3.12 [10]. The extent of dealumination monotonously increases with the partial pressure of steam.
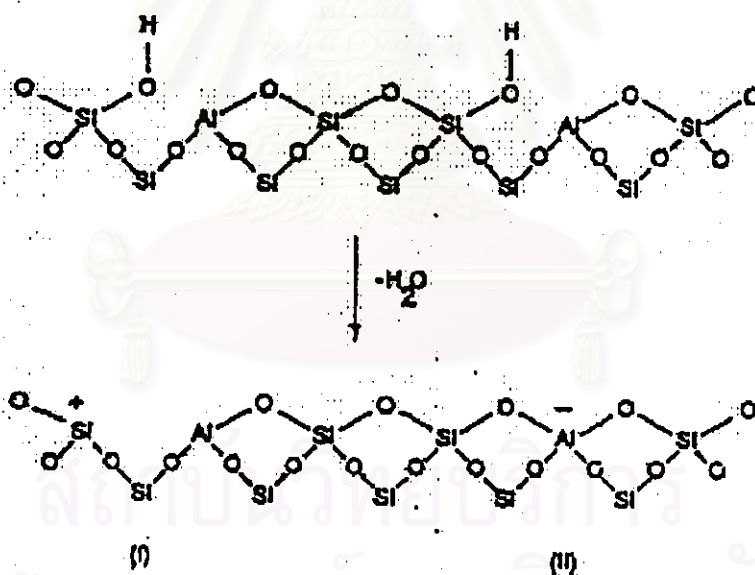

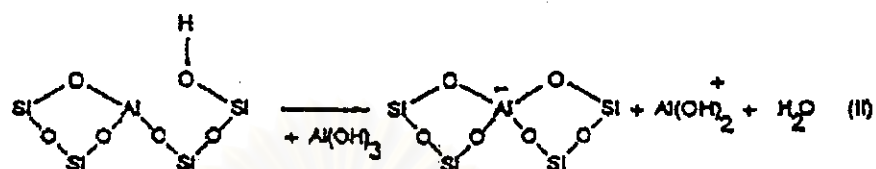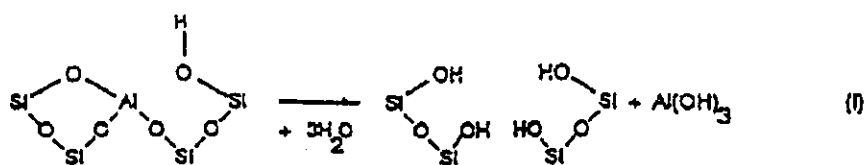Figure 3.11 Lewis acid site developed by dehydroxylation of Bronsted acid site [10].

Figure 3.12 Steam dealumination process in zeolite [10].
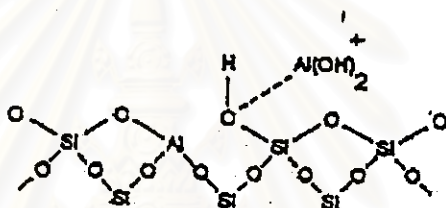

Figure 3.13 The enhancement of acid strength of OH group by their interaction with dislodged aluminum species [10].

The enhancement of the acid strength of OH groups recently proposed to be pertinent to their interaction with those aluminum species sites tentatively expressed in Figure 3.13 [10]. Partial dealumination might therefore yield a catalyst of higher activity while severe steaming reduces the catalytic activity.

3.5.3 Basic sites

In certain instances reactions have been shown to be catalyzed at basic (catio) sites in zeolites without any influence from acid sites. The best characterized example of this is that of K-Y which splits n-hexane isomers at 500 °C. The potassium cations have been shown to control the unimolecular

cracking (β - scission). Free radical mechanisms also contribute to surface catalytic reactions in these studies.

3.6 Shape - Selectivity Catalysis

Many reactions involving carbonium ions intermediates are catalyzed by acidic zeolites. With respect to a chemical standpoint the reaction mechanisms are not fundamentally different with zeolites or with any other acidic oxides. What zeolite add is shape selectivity effect. The shape selectivity characteristic of zeolites influence their catalytic phenomena by three modes; reactants shape selectivity, products shape selectivity and transition states shape selectivity [3, 11, 12]. These type of selectivity are depicted in Figure 3.14 [3].

a) Reactant selectivity
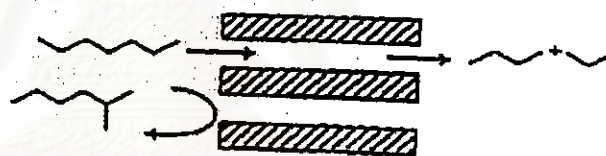
b) Product selectivity
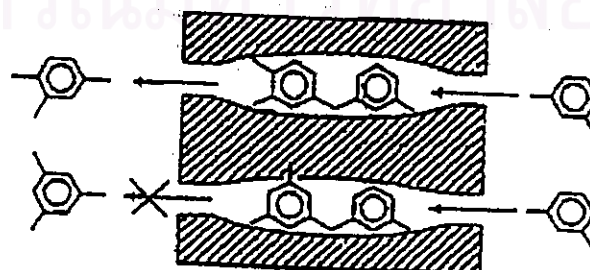
c) Transient state selectivity

Figure 3.14 Diagram depicting the three type of selectivity [3].

Table 3.3 Kinetic diameters of various molecules based on the Lennard-Jones relationship [11].

	KINETIC DIAMETER (ANGSTROMS)
He	2.60
H_2	2.89
O_2	3.46
N_2	3.64
NO	3.17
CO	3.76
CO_2	3.30
H_2O	2.65
NH_3	2.60
CH_4	3.80
C_2H_2	3.30
C_2H_4	3.90
C_3H_8	4.30
$n-C_4H_{10}$	4.30
Cyclopropane	4.23
$i-C_4H_{10}$	5.00
$n-C_5H_{12}$	4.90
SF_6	5.50
Neopentane	6.20
$(C_4F_9)_3N$	10.20
Benzene	5.85
Cyclohexane	6.00
m-xylene	7.10
p-xylene	6.75
1,3,5 trimethylbenzene	8.50
1,3,5 triethylbenzene	9.20
1,3 diethylbenzene	7.40
1-methylnapthalene	7.90
$(C_4H_9)_3N$	8.10

Reactant or change selectivity results from the limited diffusibility of some of the reactants, which cannot effectively enter and diffuse inside crystal pore structures of the zeolites.

Product shape selectivity occurs as slowly diffusing product molecules cannot escape from the crystal and undergo secondary reactions. This reaction

path is established by monitoring changes in product distribution as a function of varying contact time.
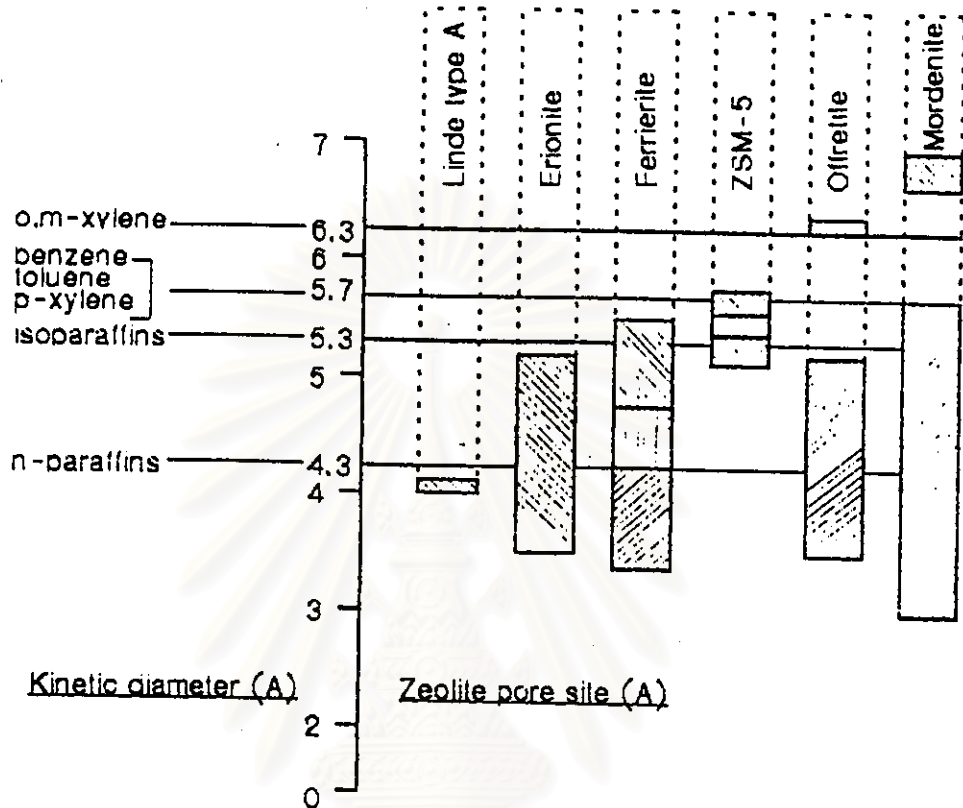

Figure 3.15 Correlation between pore size(s) of various zeolite and kinetic diameter of some molecules [11].

Restricted transition state shape selectivity is a kinetic effect arising from local environment around the active site, the rate constant for a reaction mechanism is reduced if the space required for formation of necessary transition state is restricted.

The critical diameter (as opposed to the length) of the molecules and the pore channel diameter of zeolites are important in predicting shape selective effects. However, molecules are deformable and can pass though openings which are smaller than their critical diameters. Hence, not only size but also the dynamics and structure of molecules must be taken into account.

Table 3.3 [11] presents values of selected critical molecular diameters and Table 3.4 [3] presents values of the effective pore size of various zeolites. Correlation between pore size(s) of zeolites and kinetic diameter of some molecules are depicted in Figure 3.15 [11].

3.7 Catalytic Cracking

Catalytic cracking is the most important and widely used refinery process for converting heavy oil into more valuable gasoline and lighter product. Originally cracking was accomplished thermally but the catalytic process has almost completely replaced thermal cracking because of more gasoline having a higher octane and less heavy oil and unsaturated gases are produced.

Commercial cracking catalysts can be divided into three classes: [15]
1. Acid-treated natural aluminosilicates
2. Amorphous synthetic silica-alumina
3. Crystalline synthetic silica-alumina catalysts called zeolites or molecular sieves.

Most catalysts used in commercial units today are either class (3) or mixtures of classes (2) and (3) catalysts. The advantages of the zeolite catalysts over the natural and synthetic amorphous catalysts are:
1. Higher activity
2. Higher gasoline yields at a given convrrsion
3. Product of gasolines containing a larger percentage of paraffinic and aromatic hydrocarbbons
4. Lower coke yield
5. Increased isobutane production

Table 3.4 Shape of the pore mouth opening of known zeolite structures. The dimensions are based on two parameters, the T atom forming the channel opening (8, 10, 12 ring) and the crystallographic free diameters of the channels. The channels are parallel to the crystallographic axis shown in brackets(e.g.<100>) [3].

STRUCTURE	4-MEMBER RING	10-MEMBER RING	12-MEMBER RING
Bikitaite	3.2x4.9[001]		
Brewsterite	2.3x5.0[100]		
	2.7x4.1[001]		
Cancrinite			6.2[001]
Chabazite	3.6x3.7[001]		
Dachiardite	3.6x4.8[001]	3.7x6.7[010]	
TMA-E	3.7x4.8[001]		
Edingtonite	3.5x3.9[110]		
Epistibite	3.7x4.4[001]	3.2x5.3[100]	
Erionite	3.6x5.2[001]		
Faujasite			7.4<111>
Ferrierite	3.4x4.8[010]	4.3x5.5[001]	
Gismondine	3.1x4.4[100]		
	2.8x4.9[010]		
Gmelinite	3.6x3.9[001]		7.0[001]
Heulandite	4.0x5.5[100]	4.4x7.2[001]	
	4.1x4.7[001]		
ZK-5	3.9<100>		
Laumontite		4.0x5.6[100]	
Levyne	3.3x5.3[001]		
Type A	4.1<100>		
Type L			7.1[001]
Mazzite			7.4[001]
ZSM-11		5.1x5.5[100]	
Merlinoite	3.1x3.5[100]		
	3.5x3.5[010]		
	3.4x5.1[001]		
	3.3x3.3[001]		
ZSM-5		5.4x5.6[010]	
		5.1x5.5[100]	
Mordenite	2.9x5.7[010]		6.7x7.0[001]
Natrolite	2.6x3.9<101>		
Offretite	3.6x5.2[001]		6.4[001]
Paulingite	3.9<100>		
Phillipsite	4.2x4.4[100]		
	2.8x4.8[010]		
	3.3[001]		
Rho	3.9x5.1<100>		
Stibite	2.7x5.7[101]	4.1x6.2[100]	
Thomsonite	2.6x3.9[101]		
	2.6x3.9[010]		
Yugawaralite	3.1x3.5[100]		
	3.2x3.3[001]		

3.8 Mechanism of Cracking Processes

Cracking processes were assigned to two fundamental classes;

3.8.1 Thermal cracking [16]

Thermal cracking, where free radicals (lacking one hydrogen atom on carbon atom in the hydrocarbon molecule) are intermediate species which crack by a β - scission mechanism.

The most successful present explanation of thermal cracking of hydrocarbon is Rice free radical theory as modified by Kossiakoff and Rick. This will be call the "RK-theory" as follows to explain the cracking of normal paraffin:

The normal paraffin molecule loses a hydrogen atom by collision and reaction with a small free hydrocarbon radical or a free hydrogen atom, thereby becoming a free radical itself. This radical may immediately crack or may undergo radical isomerization prior to cracking. Radical isomerization presumably occurs through a coiled configuration of a single radical, in which the hydrogen donor and acceptor carbon atom much closely approach each other. Radical isomerization is a change of the position of hydrogen atom, usually to yield a more stable radical in order of tertiary > secondary > primary free radical.

Cracking of either the original or isomerized radical then takes place at a carbon-carbon bone located in the β position to the carbon atom lacking one hydrogen atom. Cracking at the β position gives directly an alpha olefin and a primary radical (lacking one hydrogen atom on primary carbon atom); in this step no change of position of any hydrogen atom with respect to the carbon skeleton.

The primary radical derived from this step may immediately recrack at the β bone to give ethylene and another primaly radical , or it may first isomerize. In the absence of radical isomerization, only primary radicals are derived form cracking reaction of normal paraffin; primary radicals thus give only ethyllene as the olefin product. Radical isomerization reduces the amount of ethylene, but it still remains the major product. By successive recracking, the radicals ultimately are reduced to methyl or ethyl fragments. These radicals then react with feedstock molecules to produce new free radicals and are themselves converted to methane or ethane. Thus, cracking is propagated as chain reaction.

A schematic representation of octane cracking is as follows;

1. Small radical, such as CH_3, from prior cycle or from initial hydrocarbon rupture, combines with an H atom in octane to give a octyl radical and methane:

H H H H H H H H
H - C - C - C - C - C - C - C - H + CH_4
H   ·   H H H H H H
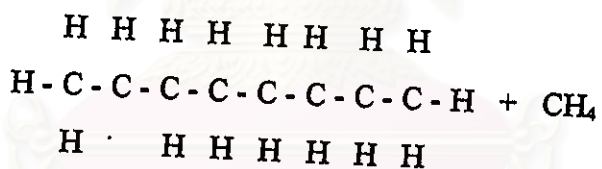
2. Octyl radical cracks beta to free valence to give propene-1 and amyl-1 radical:

H H
H - C - C = C   and
H

H H H H H
· C - C - C - C - C - H
H H H H H
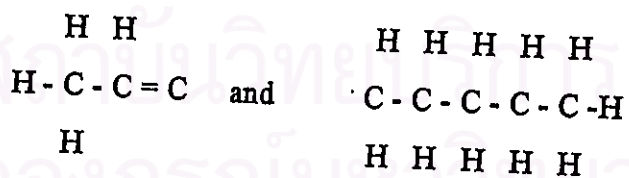
3. Amyl-1 radical cracks beta to free valence to give ethylene and propyl-1 radical; repeat process to give ethylene and methyl-1 radical, which then reacts as in step 1 to continue the chain reaction.

4. Alternatively, some of radicals in step 3 may isomerize to secondary forms, for example,

```
      H  H  H  H  H
  H - C - C - C - C - H
      H  ·  H  H  H
```
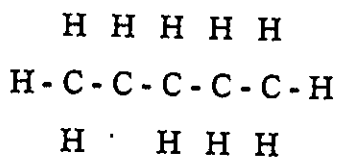
which give propylene on cracking beta to free valence. The final radical in ether 3 or 4 may be ethyl instead of methyl, which also reacts as in step 1 to continue the chain reaction.

3.8.2 Catalytic cracking [17]

Catalytic cracking process is the most important process for the production of gasoline components by the conversion of various feedstocks, such as heavier fractions, into lighter products via cracking reaction. The conversion of hydrocarbon feedstocks involves the formation of carbocations as reaction intermediates. Among the carbocations of concern for the conversion pathways of alkane and alkene, , a distinction has to be made between "alkylcarbenium ion" and "alkylcarbonium ion" , where showing in figure 3.16 [1]. Alkylcarbenium ion contain a tri-coordinateed positively charged carbon atom, the three substituents being alkyl groups or hydrogen atoms. Alkylcarbonium ions contain a penta-coordinated positively charged carbon atom, having the same type of substituents. In the carbonium ions that will be encountered, at least one of the five substituents is a hydrogen atom. The formal representation of alkylcarbonium ions used in figure 3.16 dose not violate the basic rules of organic chemistry if it is kept in mind that the five bonds of charged carbon atom contain only eight electron.

Carbocations
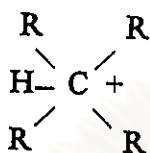
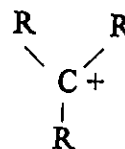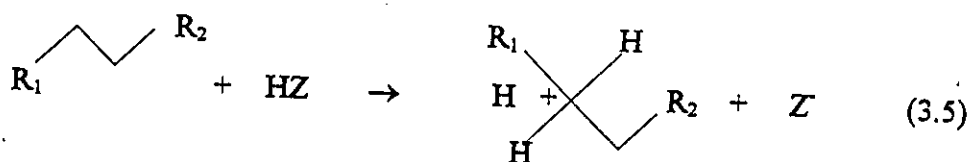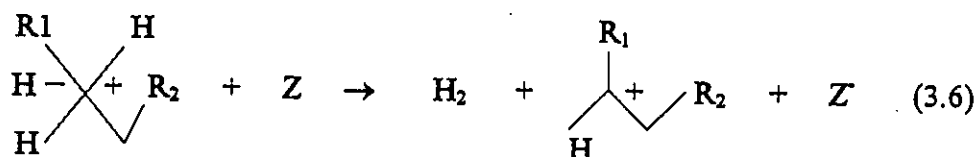alkylcarbonium ion   alkylcarbenium ion

Figure 3.16 Representation of alkylcarbenium and carbonium ions [1]

The formation of carbocations from the feedstock molecules can occur according to different mechanism, depending on the nature of feedstock and the acidic properties of the catalyst. According to Mechanism 1, a proton from the catalyst is added to the unsaturated molecules. The protonation of an alkene (olefin) by the acid zeolite (HZ) leads to the formation of an alkylcarbenium ion:
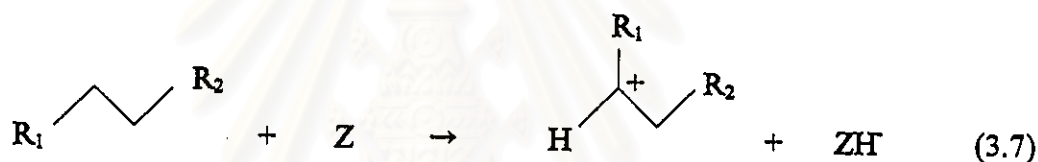

$$(3.4)$$
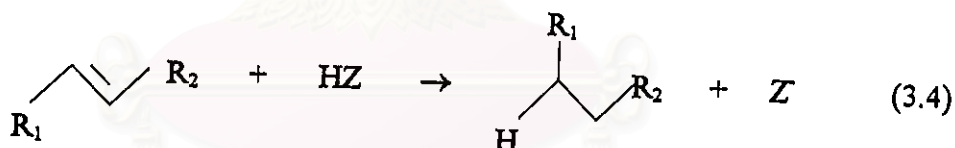
Mechanism 2 involves the addition of a proton to saturated molecule. The protonation of alkane (paraffin) leads to the formation of an carbonium ion. The carbonium ion can be transformed into a smaller carbenium ion by abstraction of an electroneutral molecule (an alkane or molecule hydrogen):
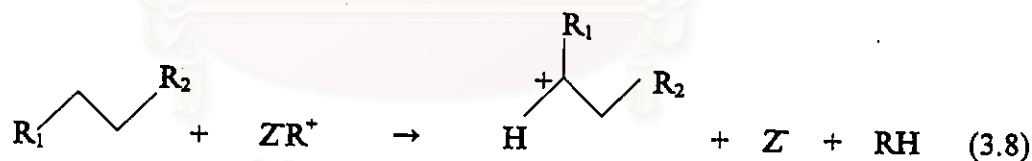

$$(3.5)$$

$$\begin{array}{c} R1 \quad H \\ H - \diagup\hspace{-0.3em}\times\hspace{-0.3em}\diagdown + R_2 \\ H \end{array} + Z \rightarrow H_2 + \begin{array}{c} R_1 \\ \diagup\hspace{-0.3em}+ \diagup R_2 \\ H \end{array} + Z \quad (3.6)$$

Mechanism 1 and 2 occur on zeolites posessing Bronsted acidity. Mechanism 1 is much faster than mechanism 2 and operates at lower temperatures.

Mechanism 3 consists of the abstraction of an hydride ion from an electroneutral feed molecules. This mechanism involves acid centers of the Lewis type:

$$R_1 \diagdown\hspace{-0.3em}\diagup\hspace{-0.3em}\diagdown R_2 + Z \rightarrow \begin{array}{c} R_1 \\ \diagup\hspace{-0.3em}+ \diagup R_2 \\ H \end{array} + ZH^- \quad (3.7)$$

A variant of mechanism 3 can occur on a carbenium ion, R+, absorbed in the zeolite pores, a phenomenon denoted as bimolecular hydride transfer:

$$R_1 \diagdown\hspace{-0.3em}\diagup\hspace{-0.3em}\diagdown R_2 + ZR^+ \rightarrow \begin{array}{c} R_1 \\ +\diagup\hspace{-0.3em}\diagup R_2 \\ H \end{array} + Z + RH \quad (3.8)$$

As demonstrated by many previous investigator [17,21,23] the cracking of n-paraffin can take place in various pathway where depend on its suitable condition.

3.8.2.1 The classical carbenium ion theory (The carbenium ion theory) [17].

The generally accepted theory of acid of acid- catalyzed cracking of paraffinic hydrocarbon date back to 1949, when Greensfelder, Voge, Good, and Thomas proposed their carbenium ion theory.

In the theory of Greensfelder, Voge, Good, and Thomas is represented in figure 3.17, cracking proceeds via a carbenium ion as an intermediate, which undergoes by β-scission to form an olefin fragment and a carbenium ion fragment. The latter ion can be transformed to a hydrocarbon fragment by hydride transfer from a paraffin molecule, which then become a new carbenium ion. In this way a reaction cycle is created. The initial carbenium ions may be formed from a feed paraffin molecule by, for in stance, hydride abstraction or by dehydrogenation and proton addition to the olefinic molecule formed.
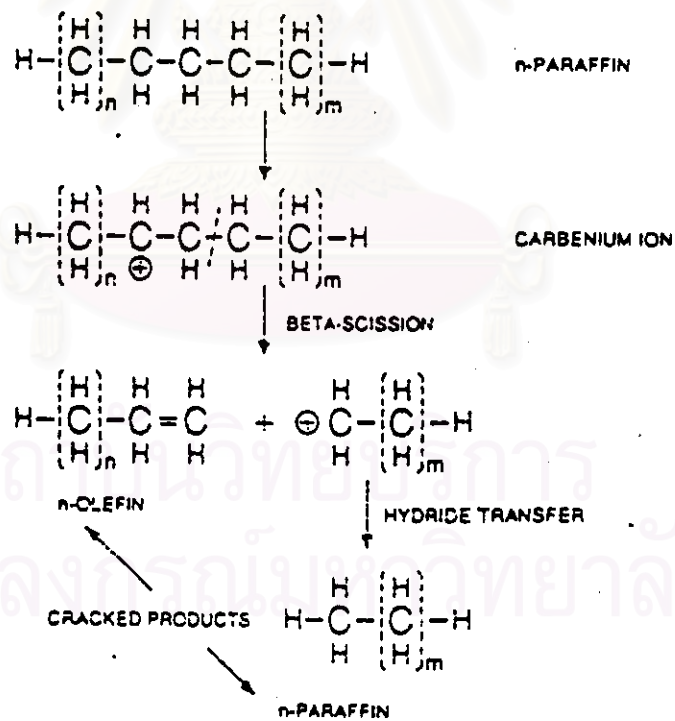

Figure 3.17 Cracking of normal-paraffin by the classical carbenium ion mechanism of Greenfelder, Voge, Good, and Thomus [17].

Main objection to this theory concerns the β-scission, a scission of the C-C bond in the β-position to the positively charged carbon atom of the carbenium ion will in the first instance produce a primary carbenium ion.

3.8.2.2 A protonated cyclopropane structure as reaction intermediate in acid-catalytic cracking [17]

A reaction mechanism based on this concept is outlined in figure 3.18, which the protonated cyclopropane ring with two alkyl groups is the intermediate of the reaction mechanism.

A 1, 3 - hydride shift from a C - atom of an alkyl group to the C - atom of the cyclopropane ring to which this group is linked, combine with a 1, 2 - hydride shift between two C - atoms of the cyclopropane ring and bond scission, leads to the tertiary carbenium ion and the linear olefin of line 5 in figure 3.18. Hydride transfer from a feed paraffin molecule to this tertiary ion produces an isoparaffin, by which the reaction is closed.

An important consequence of this reaction mechanism that the tertiary carbenium ion should have at least four carbon atom; i.e., the value of n in figure 3.18 should be at least 1. A value of zero for n implies that the initial carbenium ion would be primary one, which is very unlikely on energetic grounds.

The olefinic fragment should have at least three carbon atoms; i.e,. m' should be at least 1. A value zero for m' would imply a hydride shift from a primary carbon atom, which is energetically very unfavorable, for the same reason why hydride abstraction from a the primary carbon atom to form a primary carbenium ion is unlikely to occur.

Figure 3.18 Cracking of normal-paraffin by the non-classical carbonium ion mechanism [17].

The 1,3 - hydride shift and subsequent transformations can be regarded as a nucleophilic attach of a hydride ion originating from a beta - carbon of the alkyl group on the nearest corner atom of the cyclopropane ring, with the alkyl group minus H as the leaving group. The occurrence of these reactions as principal cracking mechanism is made more plausible when the structure of the cyclopropyl cation is considered in a three dimension form. Figure 3.19 shows a likely three - dimensional structure suggested on the basis of general chemical consideration.

It can be seem that H atom of the beta - carbon atom can be in a favorable position for nucleophilic attach on the positively charged carbon atom of cyclopropane ring. Figure 3.20 shows the position of the atoms before and after the process.

The transformation of the classical secondary carbenium ion into the protonated dialkylcyclopropane structure is not expected to involve a very high energy barrier since the energy contents of the two ions should not be 'too different.

3.8.2.3 A pentacoordinated carbonium ion as reaction intermediate in
 • acid-catalytic cracking [17]

The cracking mechanism that the protonated cyclopropane as reaction intermediate is not dominant to the cracking of n-paraffin under high reaction temperature. Under more forcing conditions, however, particularly when use is made of zeolites of high intrinsic acid strengths at relatively high temperatures, cracking of n - paraffin dose take place but leads to an entirely different product spectrum. This mechaism has been proposed by Haag and Dessau [17] and is shown in figure 3.21.
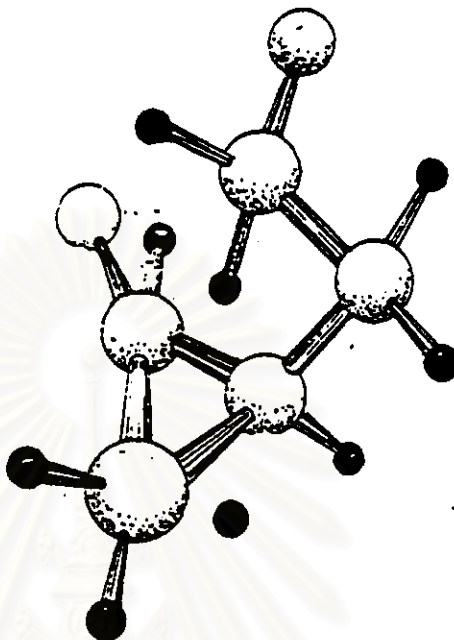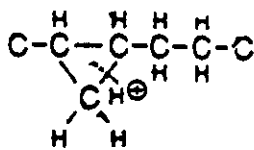
Figure 3.19 Three-dimensional representation of the protonated dialkylcyclopropane intermediate [17].
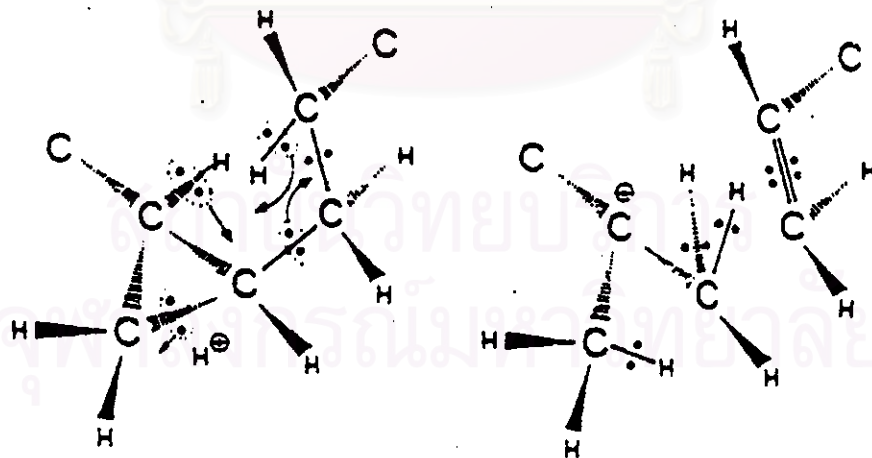

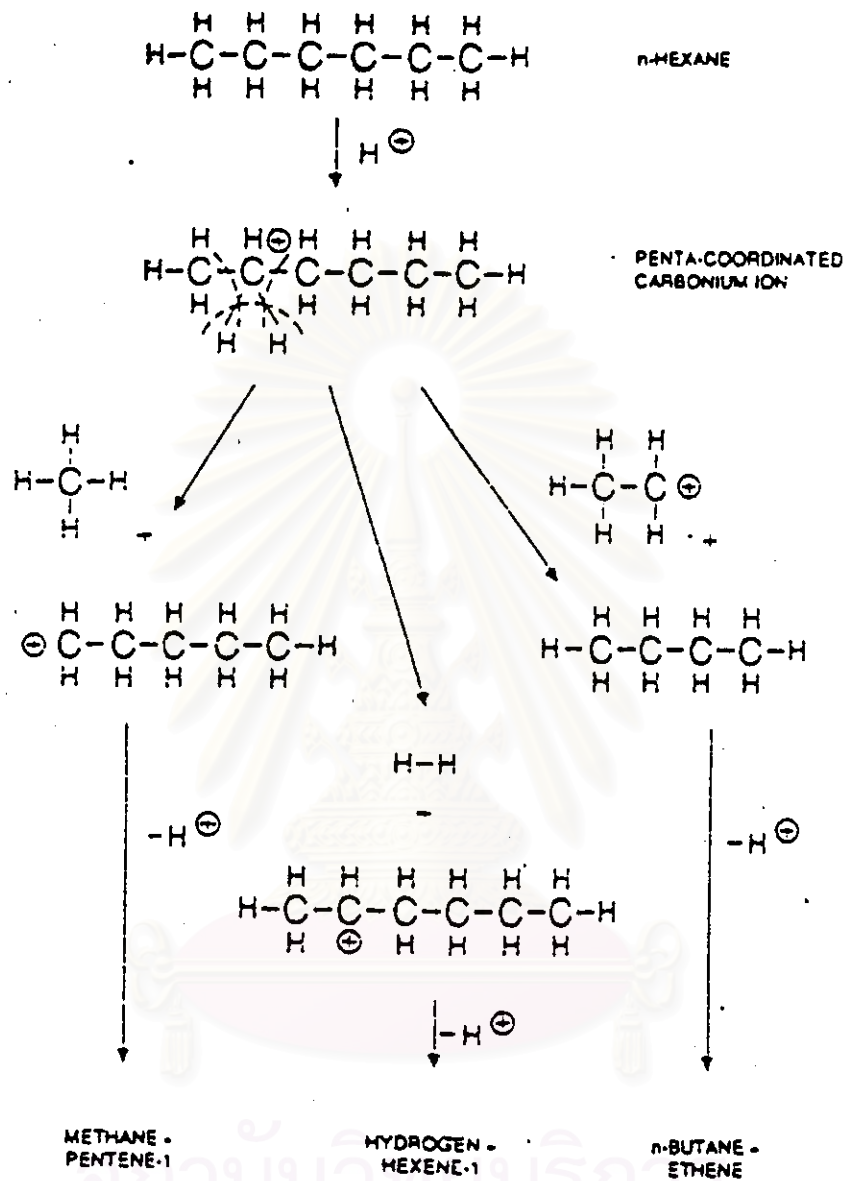**Figure 3.20** Relocation of electrons during cracking [17].

Figure 3.21 Mechanism of n-hexane cracking via a pentacoordinated carbomiun ion as intermediate [17].

This mechanism involves a pentacoordinated carbonium ion as intermediate, which is formed by proton addition to paraffin. The carbenium ion splits in the way shown in figure 3.21, yielding lower paraffins including methane and primary carbenium ions as cracked fragments.